

Evaluating uncertainties of future marine flooding occurrence as sea-level rises

Gonéri Le Cozannet, Jeremy Rohmer, Anny Cazenave, Déborah Idier, Roderik van De Wal, Renske De Winter, Rodrigo Pedreros, Yann Balouin, Charlotte Vinchon, Carlos Oliveros

▶ **To cite this version:**

Gonéri Le Cozannet, Jeremy Rohmer, Anny Cazenave, Déborah Idier, Roderik van De Wal, et al.. Evaluating uncertainties of future marine flooding occurrence as sea-level rises. Environmental Modelling and Software, 2015, 73 (November 2015), pp.44-56. 10.1016/j.envsoft.2015.07.021 . hal-01186064v2

HAL Id: hal-01186064
https://brgm.hal.science/hal-01186064v2

Submitted on 14 Sep 2015

HAL is a multi-disciplinary open access archive for the deposit and dissemination of scientific research documents, whether they are published or not. The documents may come from teaching and research institutions in France or abroad, or from public or private research centers.

L'archive ouverte pluridisciplinaire **HAL**, est destinée au dépôt et à la diffusion de documents scientifiques de niveau recherche, publiés ou non, émanant des établissements d'enseignement et de recherche français ou étrangers, des laboratoires publics ou privés.

Environmental Modelling & Software 73 (2015) 44–56

Contents lists available at ScienceDirect

Environmental Modelling & Software

journal homepage: www.elsevier.com/locate/envsoft

Evaluating uncertainties of future marine flooding occurrence as sea-level rises

Gonéri Le Cozannet [a, b, *], Jeremy Rohmer [a], Anny Cazenave [c], Déborah Idier [a], Roderik van de Wal [e], Renske de Winter [e], Rodrigo Pedreros [a], Yann Balouin [d], Charlotte Vinchon [a], Carlos Oliveros [a]

[a] French Geological Survey (BRGM), Orléans, France
[b] Université Paris 1 Panthéon-Sorbonne/Laboratoire de Géographie Physique, CNRS-UMR8591, Paris, France
[c] LEGOS-CNES, Observatoire Midi-Pyrénées, Toulouse, France
[d] French Geological Survey (BRGM), Montpelier, France
[e] Utrecht University, Institute for Marine and Atmospheric Research, Utrecht, The Netherlands

ARTICLE INFO

Article history:
Received 27 January 2015
Received in revised form
29 July 2015
Accepted 31 July 2015
Available online xxx

Keywords:
Marine flooding
Sea-level rise
Low-lying coastal areas
Global sensitivity analysis
Uncertainties
Climate change scenarios
Adaptation

ABSTRACT

As sea-level rises, the frequency of coastal marine flooding events is changing. For accurate assessments, several other factors must be considered as well, such as the variability of sea-level rise and storm surge patterns. Here, a global sensitivity analysis is used to provide quantitative insight into the relative importance of contributing uncertainties over the coming decades. The method is applied on an urban low-lying coastal site located in the north-western Mediterranean, where the yearly probability of damaging flooding could grow drastically after 2050 if sea-level rise follows IPCC projections. Storm surge propagation processes, then sea-level variability, and, later, global sea-level rise scenarios become successively important source of uncertainties over the 21st century. This defines research priorities that depend on the target period of interest. On the long term, scenarios RCP 6.0 and 8.0 challenge local capacities of adaptation for the considered site.

© 2015 The Authors. Published by Elsevier Ltd. This is an open access article under the CC BY-NC-ND license (http://creativecommons.org/licenses/by-nc-nd/4.0/).

1. Introduction

Among all adverse consequences of sea-level rise, a most immediate should be more frequent marine flooding of low lying coastal areas (Nicholls and Cazenave, 2010). This major change of coastal environmental conditions is possibly already taking place, as extreme water heights have globally risen as much as mean sea-levels (Menéndez and Woodworth, 2010; Woodworth et al., 2011; Weisse et al., 2012). As many coastal zones are already densely populated and urbanised, several studies have attempted to quantify future flood hazards (Fortunato et al., 2013) or risks (Hanson et al., 2011; Hallegatte et al., 2013). These studies have proven useful for demonstrating that future coastal flooding hazards need to be anticipated.

However, sea-level impact studies have uncertainties. Part of these originate from global sea-level rise scenarios, their regional variability, and their interactions with solid earth deformation processes (Church et al., 2013a; Nicholls et al., 2014; Slangen et al., 2014). Other are related to oceanographic processes underpinning extreme events and coastal geomorphic changes (Fig. 1; Stockdon et al., 2006; Wong et al., 2014; Cazenave and Le Cozannet, 2014; Bilskie et al., 2014). In addition, local vertical ground motions may aggravate or moderate sea-level changes at the coast (Santamaria-Gomez et al., 2012). While they are often poorly known, slight changes in their evaluation can lead to large modifications in future flood losses assessments (Woppelmann et al., 2013).

Several options are available to reduce these uncertainties. For example, accurate information on storm surges or vertical ground motions can be obtained, but at the cost of complex geophysical investigations and oceanographic studies (e.g. Brooks et al., 2007; Muller et al., 2014; Le Roy et al., 2014; Bulteau et al., 2015). Hence, the desire to maximize the social impact of future applied

* Corresponding author. French Geological Survey (BRGM), DRP/R3C, 3 avenue C. Guillemin, 45060 Orléans, France.
E-mail address: g.lecozannet@brgm.fr (G. Le Cozannet).

http://dx.doi.org/10.1016/j.envsoft.2015.07.021
1364-8152/© 2015 The Authors. Published by Elsevier Ltd. This is an open access article under the CC BY-NC-ND license (http://creativecommons.org/licenses/by-nc-nd/4.0/).

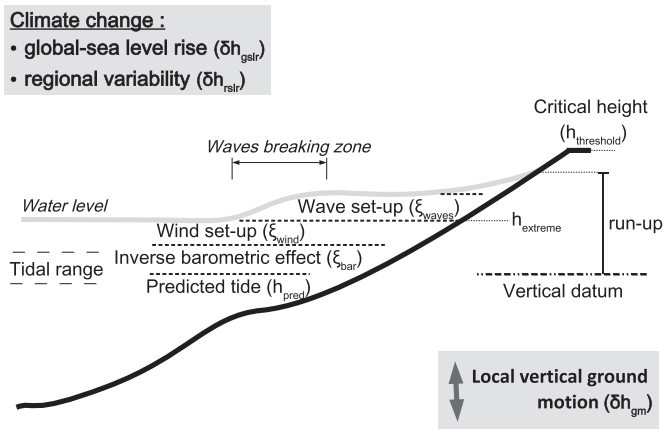


Fig. 1. Schematic synthesis of the main hydrodynamic processes involved during a storm, on an open coast unaffected by estuarine waters. Other important factors that evolve over decades are shown in grey boxes.

research raises the following questions: what is the relative importance of each source of uncertainty in the final flooding projections? Which sources of uncertainty need to be considered? Conversely, can we neglect the variability of some input parameters without affecting significantly future coastal risk assessments?

A method which is especially suitable to answer these questions is the variance-based global sensitivity analysis (Sobol', 2001; Saltelli et al., 2008; Norton, 2015). Given a model with uncertain input parameters, this approach quantitatively assesses the contribution of each uncertain model input on the variability of their output. Contrary to the "One-factor-At-a-Time" (OAT) technique, variance-based global sensitivity analysis (GSA) consider that all uncertain input parameters can vary together (i.e., in a global manner). Hence, GSA allows to identify which sources of uncertainty contribute the most to the output variability and which input parameters are insignificant and can be eliminated (Saltelli and Annoni, 2010). Unlike OAT, GSA explicitly quantifies how interactions between input factors affect the variability of the final results, and no a-priori assumption needs to be done on the structure of the mathematical model of interest (Saltelli, 2004).

While variance-based sensitivity analysis is not new, there are surprisingly few applications, whether in the field of future coastal changes (see Chu-Agor et al. (2011) for an application to wetland ecology) or in the wider domain of climate change impacts uncertainty (Saltelli and D'Hombres, 2010; Anderson et al., 2014). Instead, coastal impact studies have rather evaluated the uncertainties by considering a few possible values of the input parameters independently (OAT technique), and often focused on the climate-driven part of uncertainties only. In such cases, only a part of the model outcome variability is considered, and the actual ranking of the relative importance of uncertainties is difficult (Saltelli, 2004; Norton, 2015). Furthermore, few studies incorporate probabilistic sea-level scenarios in impact assessments, which can lead to underestimations of potential impacts (Purvis et al., 2008). Finally, the temporal evolution of sea-level rise is rarely addressed. This raises difficulties as recommended approaches toward adaptation require input information on the temporal dynamics of future changes (e.g., Lempert and Schlesinger, 2000; Hallegatte, 2009).

To summarize, there is a need for probabilistic information on future coastal flooding occurrence, using objective and robust measures of the uncertainties importance, and addressing the temporal dimension of expected changes. This paper sets up a model evaluating how the probability of extreme marine flooding evolves over the time under different sea-level rise scenarios. We use the sea-level rise scenarios provided by IPCC (Church et al., 2013b) for different representative concentration pathways (RCP; see Table 1). The model is designed to be easily applicable for a wide range of coastal sites, including those where little is known regarding local coastal processes. The contribution of each source of uncertainty and its evolution over time is evaluated by means of a global sensitivity analysis (section 2). We apply the approach to a local low-lying coastal urban area exposed to storm surge and waves in the north-western Mediterranean and evaluate the relative importance of each source of uncertainty in order to define priorities for future applied research for this site (section 3). Finally, we discuss the usefulness and limitations of our approach for understanding uncertainties on coastal climate change impacts, and examine the implication of our results for adaptation and mitigation of climate change (section 4).

2. Method

2.1. Marine flooding in urban environment

Marine flooding generally occurs during extreme events induced by hydro-meteorological storms. During such storms, the water level can rise above the predicted tide due to (Fig. 1): (1) reduced atmospheric pressures (inverse barometric effect), (2) strong winds, possibly leading to accumulation of water in shallow areas (wind set-up), and (3) a rise of sea-level due to wave breaking (wave set-up). Importantly, wave set-up is different from the instantaneous effect of each individual wave, which cumulates with the previous effects to reach an altitude called run-up. The wave set-up may reach up to several tens of centimetres, depending on offshore waves patterns and coastal submarine slopes (Stockdon et al., 2006). Hence, the actual water-level heights at the coast can be highly sensitive to changes in the near-shore coastal bathymetry induced by sediment transport processes. When relevant, other effects such as the influence of an estuary or sea-level seasonal or inter-annual variability must be taken into account for accurate coastal flooding assessment.

Marine flooding may involve processes such as storm-induced sediment transport and breaching of coastal dunes. However, in coastal urban environments, damaging marine flooding often occurs as soon as the highest water levels or waves exceed a critical threshold ($h_{threshold}$), corresponding to the height of coastal defences or low walls (Idier et al., 2013b). Here, we consider the situation where coastal flooding becomes especially damaging, that is, when mean water levels (and not only the run-up induced by highest waves) exceed this critical level and cause rapid rise of water level behind coastal defences (André, 2013). Therefore, under the present day's conditions and at a given location x, damaging marine flooding occurs as soon as:

$$h_{threshold}(x) < h_{pred}(x) + \xi_{bar}(x) + \xi_{wind}(x) + \xi_{waves}(x) \quad (1)$$

where h_{pred} is the altitude corresponding to the predicted tide and

Table 1
Overview representative concentration pathways and likelihood to meet the 2° C target, as established by IPCC. The 2° C target corresponds to a rise of temperatures in 2100 with respect to the pre-industrial era.

Scenario	Likelihood to exceed the 2° C target (from IPCC)
RCP 2.6	unlikely (medium confidence)
RCP 4.5	more likely than not (medium confidence)
RCP 6.0	likely (high confidence)
RCP 8.5	likely (high confidence)

ξ_{bar}, ξ_{wind} and ξ_{waves} are the additional water levels resulting from barometric and wind effects and the wave set-up. In coastal sites exposed to waves and unaffected by estuaries, this approach provides a good approximation of observed water levels.

Let us now consider marine flooding in the future. Other terms that modify relative mean sea-level (i.e. with respect to the coast) must be considered. This includes: (1) the rise of global sea-level induced by future climate change (hereafter: δh_{gslr}), regional deviations to the global mean (δh_{rslr}), and local ground motions (δh_{gm}). More details on these processes are provided in section 3.2 and a comprehensive review is provided in Church et al. (2013a). Hence, Equation (1) becomes:

$$h_{threshold}(x,t) < h_{pred}(x,t) + \xi_{bar}(x,t) + \xi_{wind}(x,t) + \xi_{waves}(x,t) + \delta h_{gslr}\left(t, s_{rcp}, z_{max}(t)\right) + \delta h_{rslr}(x,t) + \delta h_{gm}(x,t) \quad (2)$$

All these terms can change in the next decades to centuries: mean and extreme sea-level pressures, winds or waves (hence, ξ_{bar}, ξ_{wind} and ξ_{waves}) can be affected by a changing climate (Wong et al., 2014; Hemer et al., 2013). Sedimentary changes induced by natural processes, anthropogenic actions or climate change can also affect bathymetric slopes, and, therefore, ξ_{waves}. Therefore, all terms in Equation (2) are not only function of the position (x), but also of the time (t). As a first approximation, we consider that only global sea-level rise is affected by climate change scenarios s_{rcp}. The upper-bound for global sea-level rise projections ($z_{max}(t)$ in Equation (2)) is an important additional source of uncertainties due to unknowns in polar ice-sheets processes (Church et al., 2013b; Jevrejeva et al., 2014).

To summarize, Equation (2) provides a simple condition for damaging marine flooding and applies as a first approximation in low lying coastal urban or peri-urban environments, where a critical threshold can be identified in coastal defences heights.

2.2. Global sensitivity analysis in the context of future urban marine flooding

Each term in Equation (2) is uncertain (Nicholls et al., 2014). Let us assume that this uncertainty can be modelled by appropriate probability distributions. In this case, it becomes possible to evaluate how the probabilities of critical threshold exceedance evolves over the time simply by using Equation (2). In this study, we focus on the yearly probability of exceedance (hereafter F_t), which is the inverse of the return period for flooding. This criterion is commonly used for risk assessment and coastal defence design (e.g. Tawn, 1992; Miller et al., 2014), and even for individual's resettlement decisions (survey of Meur-Ferec et al., 2010; presented in Idier et al., 2013b).

The uncertainties of the outcome parameter F_t depend on the probability distribution of the input parameters $(X_i)_{i=1..10} = (h_{threshold}(x,t), h_{pred}(x,t), \xi_{bar}(x,t), \xi_{wind}(x,t), \xi_{waves}(x,t), s_{rcp}, z_{max}(t), \delta h_{gslr}(t,s_{rcp},z_{max}(t)), \delta h_{rslr}(x,t), \delta h_{gm}(x,t))$. To provide a quantifiable measure of the relative importance of each of eight contributing input factors to the global uncertainty, a common approach consists in evaluating how the variance of the model outcome is affected by the variability of the input parameters (Sobol', 2001; Saltelli, 2004; Saltelli et al., 2008; Norton, 2015). To ensure that the full variability of the model outcome is analysed, the recommended practice consists in considering that all parameters can vary simultaneously over their full range of variability (Saltelli et al., 2008). This approach is called global sensitivity analysis.

The principle of global sensitivity analysis is to separate the variance of the model outcome into several terms, corresponding to the effects of input parameters (here assumed to be statistically independent) and their interactions (Sobol', 2001; Saltelli et al., 2008). A sensitivity measure is defined by evaluating the part of the variance of F_t attributed to the possible values of X_i, namely the variance of the conditional expectation normalized by the unconditional variance of F_t. This defines the first-order Sobol' indices:

$$S_i = \frac{Var(E(F_t|X_i))}{Var(F_t)} \quad (3)$$

where E is the expectation operator. Equation (3) represents the contribution of X_i alone to the uncertainty on F_t. In this sense, it is the main effect of X_i, and it is used to rank the importance of the different X_i (Saltelli, 2004; Saltelli et al., 2008).

Higher order Sobol' indices $S_{i..j}$ represent the combined effects of the independent parameters $X_i..X_j$:

$$S_{i..j} = \frac{Var\left(E\left(F_t|X_i..X_j\right)\right)}{Var(F_t)} - S_i - .. - S_j \quad (4)$$

$S_{i..j}$ are called interaction terms, as they represent a fraction of the normalized variance that can only be reached by varying at least two of the independent input parameters (Saltelli et al., 2008). For example, this can correspond to ranges of F_t that can only be obtained for sea-level rise and wave set-up values, which are both higher than their average values.

In practice, there is a large number of indices to handle, and the analysis is often restricted to the total effect index defined as the sum of its main and all higher order effects where X_i is involved:

$$S_{Ti} = 1 - \frac{Var(E(F_t|X_{-i}))}{Var(F_t)} \quad (5)$$

where X_{-i} includes all X_j except X_i. The total effect index is a measure of the total impact of an input parameter to the variance of the results, that is, its main effects plus all its interactions with other input parameters (Homma and Saltelli, 1996). When the total effect index is close to zero, the parameters can be set to a fixed value without changing the variance of the model outcome.

The most difficult task is to elaborate adequate probabilistic representations of the uncertainties for each input parameter in Equation (2). First, an appropriate probability law must be selected. Then, the probability density function (PDF) or the cumulative distribution functions must be fitted to the information available. This information can partly exist in a probabilistic form, but should also incorporate complementary observations and model results. The final probabilistic representation of each parameters will depend on the coastal site considered, but also on the degree of knowledge by which each process is known in the area of interest.

3. Application at a local coastal site

3.1. Coastal site

To test the approach in a real case, we select an urban coastal site located on the French coast of the gulf of Lion in the north-western Mediterranean (Fig. 2). The area has been affected by several severe storms in the recent past (Gervais et al., 2012; De La Torre et al., 2013). In particular, the 1982 storm caused flooding and damages in the place of interest (Vinchon et al., 2011b).

Previous investigations on future coastal hazards undertaken in this region highlighted the high spatial variability of potential climate change impacts (Vinchon et al., 2009; Le Cozannet et al., 2013). They identified distinct profiles for coastal cities, the most vulnerable being located on low-lying Holocene sand barrier,

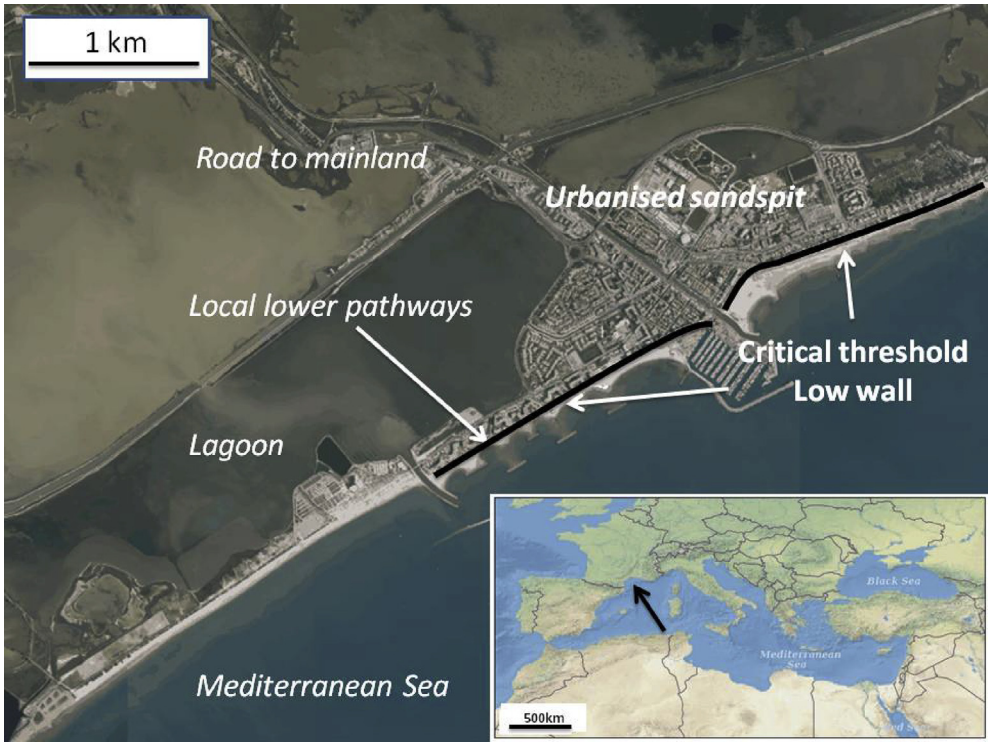


Fig. 2. Location of the coastal site of interest and of the critical threshold (Data: Infoterre/BRGM/IGN).

whereas cities on rocky outcrops are not directly threatened. Hence, the critical "hotspots" of climate change impacts are relatively well identified. Conversely, much less is known about the periods of time by which these changes should occur. The urban infrastructures of our test site is one of these hotspots. It is located on an almost continuous low-lying sand barrier which separates the sea from the lagoons.

3.2. Probabilistic modelling of input parameters

For several terms of Equation (2), ranges of possible values can be found in the literature (Table 2). Available geodetic data (levelling data, permanent GPS, tide gauge) and the geological investigations show no evidence of coastal vertical ground motions at this coastal site. Hence, the contribution of δh_{gm} is not considered here. While changes or variability in marine storm surge climate can be important in many locations (e.g., Chu-Agor et al., 2014), Ullmann (2008) showed that most of the changes in marine flooding hazards will be due to sea-level rise in the western Mediterranean sea, so that other climate change impacts to tides, surge and waves are second order effects. Finally, we consider that the critical threshold $h_{threshold}$ does not change over the time, in order to evaluate the degree of protection offered by the already existing low walls under different sea-level rise scenarios. With these site-specific simplifications, Equation (2) becomes:

$$h_{threshold} < h_{extreme} + \xi_{waves} + \delta h_{gslr}\left(t, s_{rcp}, z_{max}(t)\right) + \delta h_{rslr}(t) \tag{6}$$

where $h_{extreme} = h_{pred} + \xi_{bar} + \xi_{wind}$ represents the maximum water level in the local terrestrial framework.

Table 2 summarizes the probability distributions used to model the uncertainties on this site. We use a Beta law to represent global sea-level rise scenarios (see Figs. 3 and 4, and Appendix A), a uniform distribution to represent the uncertain upper limit of global sea-level rise (called "high-end scenario" hereafter), triangular laws for regional sea-level rise variability (Appendix B) and a uniform law for the wave set-up. A Pareto law fitted to uncertain heights of centennial and decennial events is chosen to represent our uncertainties on extreme events. The heights of centennial and

Table 2
Overview of the probability distribution functions used in this paper to model the variability of input parameters. Details are provided in section 3.2. The table includes key bibliographic references used for assessing the parameters of the probability density functions.

Parameter	Description	Selected boundary values	Probabilistic model	Reference
$h_{threshold}$	Critical threshold	2.15 m above the vertical reference	Fixed at 2.15 m	Idier et al. (2013b)
$h_{extreme}$	Offshore extreme water levels	Values ranging from 1.3 to 2 m for the centennial event	2-parameters Pareto distribution	Yates et al. (2011)
ξ_{waves}	Wave setup	0.4 m–0.8 m	Uniform distribution	Gervais (2012)
$h_{gslr}(t)$	Global sea-level rise	Low- and high-end scenarios (see text)	Beta distribution	Church et al. (2013a)
$h_{rslr}(t)$	Sea-level variability	Regional bias ±0.1 m (present) to ±0.25 m (after 65 yrs)	Triangular distribution	Church et al. (2013a) and Slangen et al. (2014)
s_{rcp}	Climate change scenario	RCP 2.6, 4.5, 6.0 and 8.5	Uniform discrete distribution	Church et al. (2013a)
$z_{max}(t)$	High-end sea-level rise scenario	1.5–3 m by 2100	Uniform distribution	e.g., Jevrejeva et al. (2014)

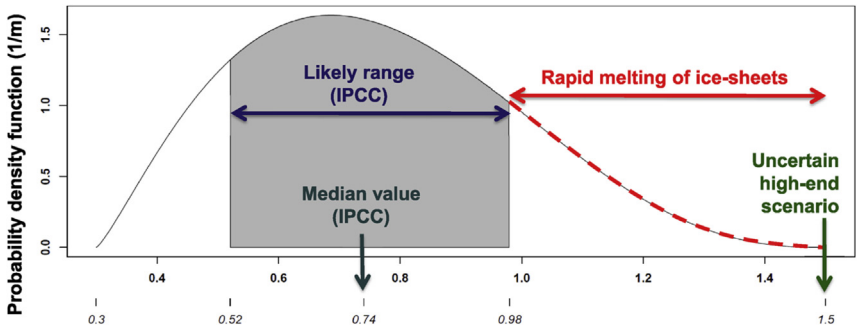


Fig. 3. Shape of the Beta probability density function used for representing sea-level rise by 2100 for RCP 8.5. In this case, $\alpha = 2.25$ and $\beta = 3.64$. Note that α and β vary depending on the upper and lower bound, likely range and median values at each timestep and for each climate change scenario. High-end scenarios represent the upper limit of sea-level rise projections.

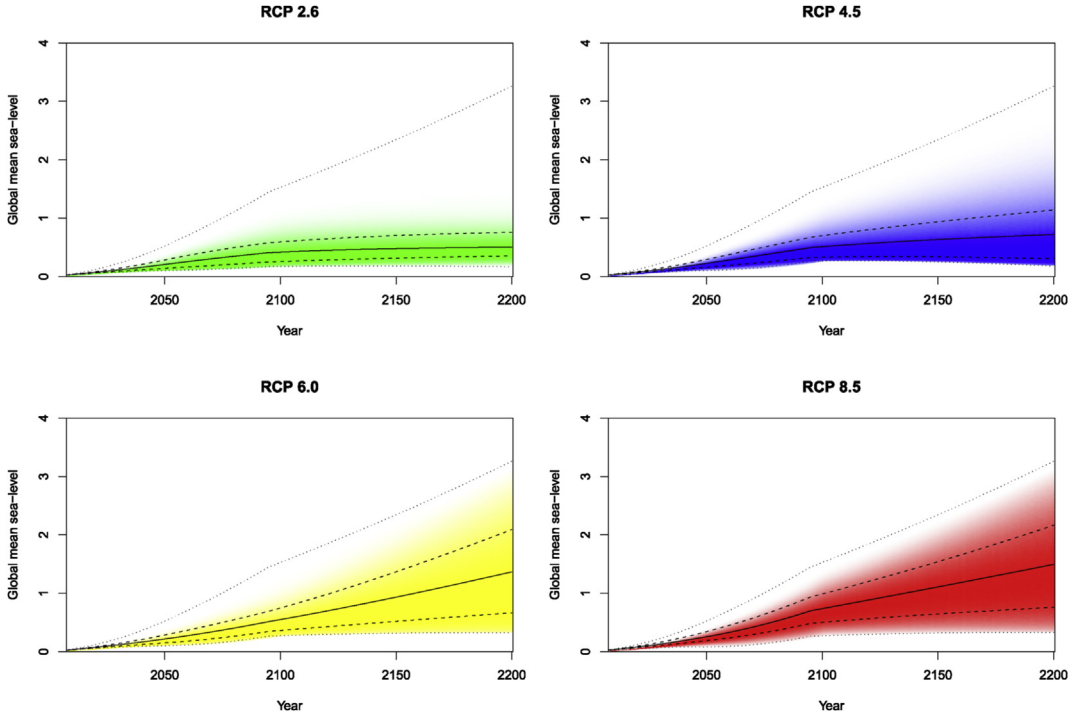


Fig. 4. Global sea-level rise scenarios used in this study. Solid, dashed and dotted lines correspond to the median, to the likely range likely (66%) and low- or high-end scenarios respectively. These values are used to define the global sea-level rise probability density function (see Fig. 3), shown here at each time step by the intensity of the colour. They are based on the IPCC and complementary knowledge (see Appendix A). (For interpretation of the references to colour in this figure legend, the reader is referred to the web version of this article.)

decennial events follow uniform laws bounded by our evaluation of possible extreme water levels return periods (Appendix C). The appendixes provide the details for each process, including: the motivations for selecting the PDFs listed in Table 2, the observations, models and reports that support the values, the assumptions made, and, finally, the methods developed to calculate the parameters of the selected PDFs.

3.3. Computational approach to evaluate time-evolving uncertainties

Fig. 5 summarizes the computational approach for random simulations of the yearly probability of exceedance F_t. Sobol' indices are computed independently at each time step (i.e. each year).

The method to compute first-order and total-order indices is well established (Saltelli et al., 2010). To reduce computational costs, a quasi-Monte-Carlo approach is preferred over purely random simulations. We use the Sobol' sequence of quasi-random numbers (Sobol', 1967), which allows to fill more evenly the hypercube of normalized input parameters and to reduce the convergence time. To calculate the Sobol' indices, we use the R implementation (R Core Team, 2014) of the Saltelli et al. (2010) algorithm, based on the Jansen (1999) formulation.

Here, an additional level of complexity resides in the nature of some input parameters, which are actually the parameters of probabilistic laws. In particular, this is the case for the global sea level rise h_{glsr} which is assumed to follow a Beta law whose parameters α and β (see Appendix A) depends on the choice of the climate change and high-end scenarios (s_{rcp} and z_{max}). This makes the variability in h_{glsr} conditioned on s_{rcp} and z_{max}. Hence, the sensitivity index of h_{glsr} depends on the climate change and high-end scenarios, which prevents us from directly using expressions of the Sobol' indices as traditionally used. This issue has extensively

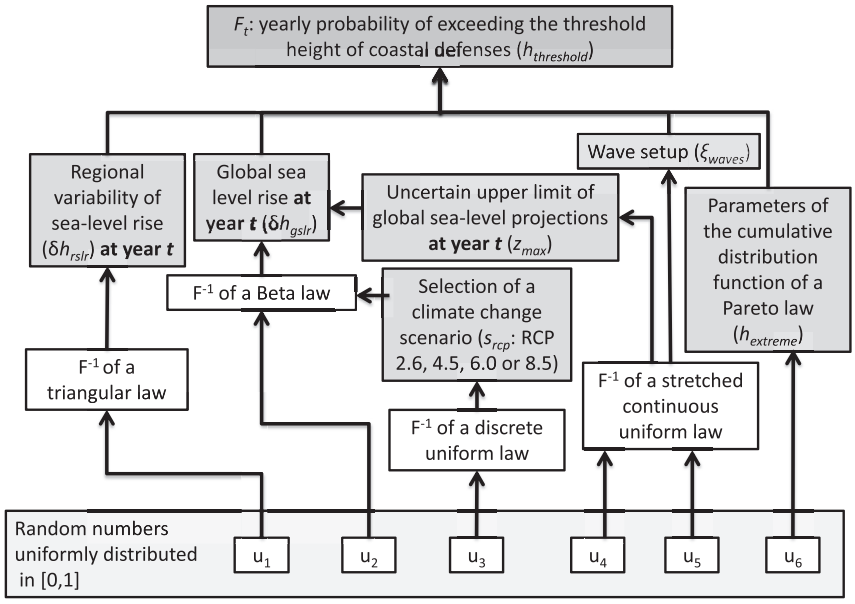


Fig. 5. Computational approach for computing random samples of the probability of exceedance of the critical threshold height of coastal defences. To perform the sensitivity analysis, this procedure is called 40000 times each year from 2005 to 2200, with input parameters u_1 to u_6 following a Sobol' sequence of 5000 quasi-random numbers.

been discussed by Sankararaman and Mahadevan (2013). Following their approach, we rely on the use of auxiliary random variables denoted $(u_i)_{i=1..6}$, which are uniformly distributed in the range [0,1], and are related to the actual parameters using the inverse probability functions. In the example of the global sea-level rise, h_{glsr} can be then be sampled using $F^{-1}(u_2|u_3, u_4)$ with F^{-1} the inverse cumulative distribution function of the Beta law (see Fig. 5 for notations). The advantage is that u_2, u_3 ans u_4 can be sampled independently from each other and a sensitivity index can be assigned to both of them using the traditional procedure.

The number of simulations required to compute the Sobol' indices reaches $N(k + 2)$, where k is the number of parameters (here, 6) and N the number of iterations necessary to converge to a required precision. In the present case, the lowest convergence is obtained when all parameters have a significant contribution to the global uncertainties, that is, by 2080–2100. Our results were obtained with $N = 5000$, which allows to estimate Sobol' indices with a precision in the order of 10^{-3} or better.

3.4. Variance of model outcome and uncertainty ranking

Once the method has been applied, the results allow to identify:

- the temporal evolution of the probability of exceedance of coastal defences for each climate change scenario (Fig. 6),
- variance-based measures of the relative importance of each input parameter (Fig. 7),
- parameters whose total index is close to zero and can be set to a fixed value without much impacts for the final results (i.e., without affecting significantly the variance of the model outcome) (Fig. 8). This last figure is discussed in depth in Subsection 4.2.

Fig. 6 shows how the yearly probability of exceedance of the critical threshold F_t evolves over the time, assuming no rise of coastal defences. Note that to qualify the range of uncertainties in this figure, we use the common definitions adopted by IPCC. For all four climate change scenarios, F_t rises slowly up to 2050. After 2050, the four scenarios lead to very different situations: in the case of RCP 2.6, the rise of F_t is limited, with more than 95% chance that marine flooding return periods remains below 2 years. Section 4.3 discusses the implications of such changes for individual relocation decisions. Conversely, the same critical threshold has more than a 50% chance to be exceeded at least once per year by 2150 for scenarios RCP 6.0 and 8.5. This is consistent with IPCC sea-level rise scenarios, which remain similar up to 2050 and then differ(Church et al., 2013a).

The uncertainties are very large: this is shown by the large spread of likely and extremely likely ranges of F_t in Fig. 6, as well as by the standard deviation of model outcomes in the lower part of Fig. 7. The relative importance of these uncertainties can be evaluated through the first order Sobol' indices obtained from the global sensitivity analysis (Fig. 7). Note that the sum of all first and higher order Sobol' indices is equal to 1 (see Equation (3)), whereas the sum of the total effect indices is larger than 1 as soon as there are non-zero interactions terms (Fig. 8).

At present, regional to local surge processes remain the largest source of uncertainties, that is, those related to the wave set-up, wind set-up and inverse barometric effects. After 2050, an increasing part of the uncertainties comes from global sea-level rise. The effect of the climate change scenario to the variance of the model outcomes grows after 2080 only. The variability of sea-level rise has an important contribution to the uncertainties from the coming decades to 2150. The upper limit of global sea-level rise (high-end scenario) has a limited contribution to the variance of the model outcome. This was expected as high-end scenarios mainly affect the tail of the distribution of global sea-level rise, whereas global sensitivity analysis provides variance-based measures.

The relative importance of the interaction terms (defined as one minus the sum of the main effects of all input factors) grows rapidly during the first 60 years, then decreases by the end of the 21st century, and finally remains almost constant beyond 2100 (Fig. 7). This behaviour can be explained by threshold effects: Fig. 6 shows that the range of values potentially taken by the outcome parameter F_t increases until the yearly probability of flooding reaches 1. This happens first for worst-case combinations of the input parameters in the case of climate change scenario RCP 8.5, and, later, for RCP 6.0 and RCP 4.5. Conversely, this stage is never met for RCP

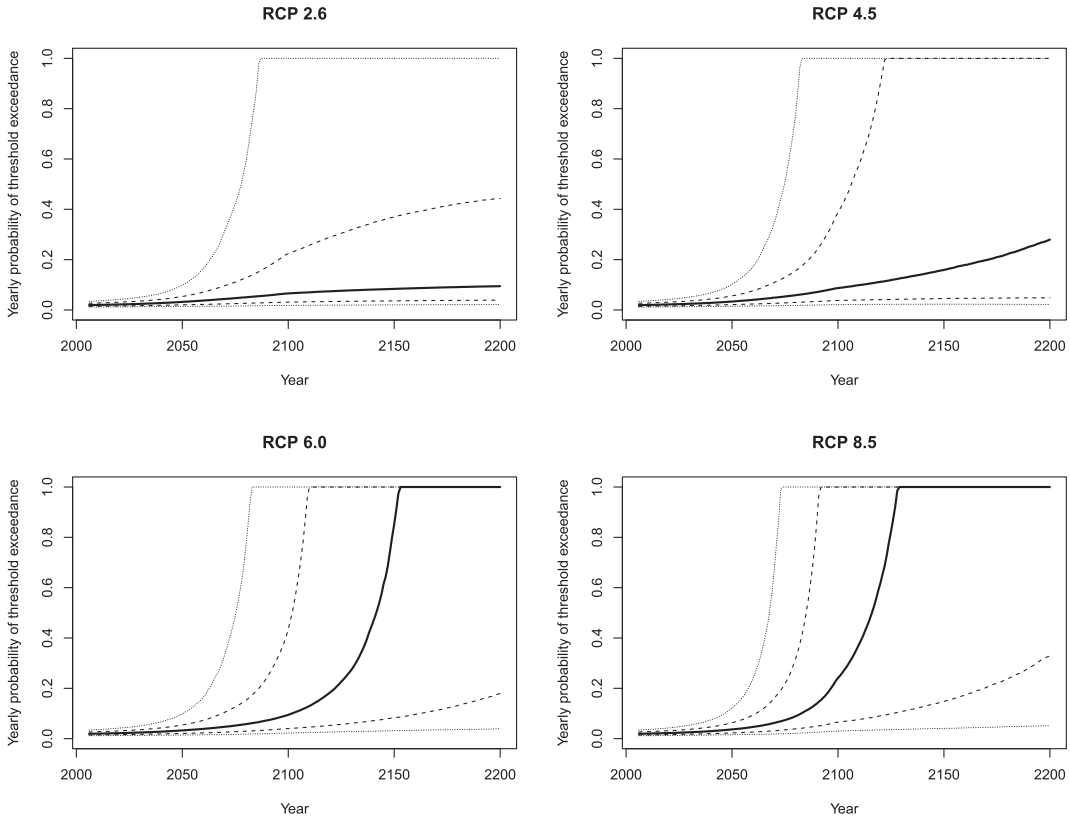


Fig. 6. Evolution of the probability of storm-induced sea-level exceedance uncertainties over time for the four climate scenarios. Solid, dashed and dotted lines correspond to the median, to likely (66%) and extremely likely (95%) ranges respectively. Note that the y-axis represent probabilities, which are therefore dimensionless.

2.6. As soon as the upper limit of F_t is reached, combinations of worst-case input values no longer increase the maximum values of the model outcome. Non-bounded outcome parameters such as the costs induced by future flooding could lead to a monotonous growth of the interaction terms, depending on the geomorphology and exposed assets at the site considered.

To summarize, the results presented in this section show that as expected, the relative importance of the sources of uncertainties change over the time: local coastal processes are the most important during the 1st part of the 21st century, whereas uncertainties

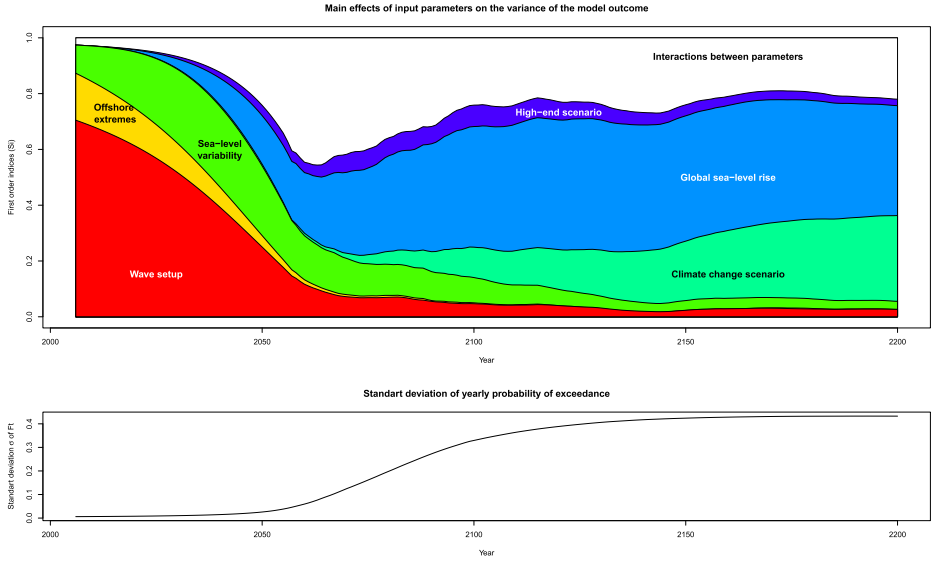


Fig. 7. Upper graph: evolution of the first-order Sobol' indices over the time, for the six input parameters selected in this paper. These indices correspond to contribution of each input parameter to the variance of the model outcome, obtained by averaging the effects of other parameters. They can be used to rank the sources of uncertainties, in the sense that the largest the first-order index, the largest its main effect to the variance of the model outcome. The lower part of the figure provides the standard deviation of the yearly probability of exceedance (F_t). It shows that uncertainties grow as time evolves, with a strong acceleration starting in 2070. This is consistent with sea-level scenarios provided by Church et al. (2013a). Note that the variables represented on the y-axis are adimensional.

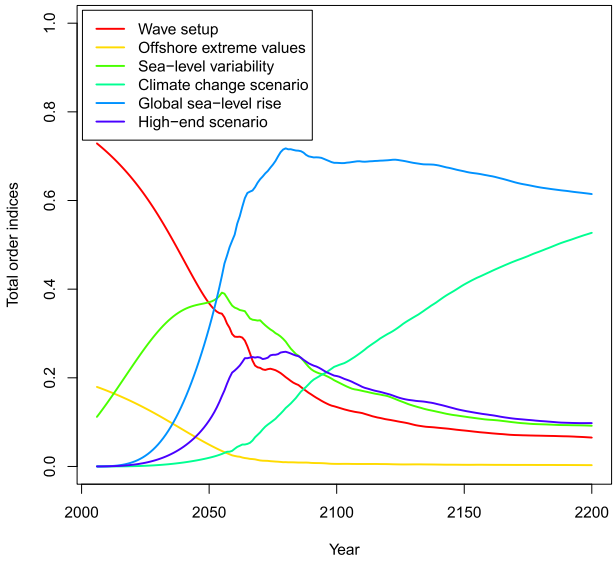


Fig. 8. Evolution of total-order indices over the time, for the five input parameters selected in this paper. These indices correspond to the total variance of the model outcome obtained by each input parameter, including the interactions with all other input parameters.

of future sea-level rise scenarios largely dominate beyond 2080. The relative importance of sea-level variability reaches its maximum from 2020 to 2070. While these results could be roughly anticipated qualitatively at this specific site, the approach presented here provides quantified evidences of these points.

4. Discussion

4.1. Applicability of the method in other coastal contexts

In this location, Yates et al. (2011) previously examined errors in 2100 erosion and submersion hazard assessment. They performed a sensitivity analysis considering input factor varying independently (OAT technique). Their results shows that uncertainties related to future sea-level rise scenarios and local coastal processes are important. However, the comparison of their relative importance is difficult, because the limited number of simulations is not necessarily representative of the actual probability density distribution of the input parameters. Moreover, the interaction terms can not be evaluated in this study. Here, the global sensitivity analysis overcomes these two issues by providing a decomposition of the variance of the model outcome, where a measure of the relative importance of each input factor and of their interactions can be isolated.

Provided enough knowledge is available regarding the variability of each input factor, the method can be applied in other coastal locations. Necessarily, the exercise of converting the existing modelling results, synthesis and expertise into probabilistic density functions is partly subjective. Future research would be useful to improve the probabilistic modelling of the input parameters such as global and regional sea-level rise, local and regional coastal processes and — when relevant — coastal ground motion. However, we argue that when defining these functions, the priority should be given to obtaining fair representations of the variability of all process, rather than undertaking a complex detailed modelling of a few of them, with little impact to the final ranking.

Finally, two lines of improvement can be proposed regarding the methods for global sensitivity analysis. First, in this application, we assumed that the five input factors are independent, whereas some could be correlated in reality. For example, tides and sea-level rise display some dependency in some locations (Pickering et al., 2012). For sites where such dependencies can be quantified, independent groups of correlated variables can be defined (Jacques et al., 2006), or extended definitions of the Sobol' indices can be used (e.g., Mara and Tarantola, 2012). Depending on the application and on the significance of the correlation found, this issue can deserve some attention. Second, we conducted separated sensitivity analysis at each time step (considered independent from each other). Yet, this might lead to redundancy (see discussion in Campbell et al., 2006), because we did not take advantage of the strong relationship between responses from one time step to the next one, i.e. the output is not scalar, but a time-varying function. Extensions of Sobol' indices in the case of functional output should be used in the future (Gamboa et al., 2014).

4.2. Defining research priorities based on the global sensitivity analysis results

Depending on the period considered, Fig. 8 defines priorities for future research in this area. Beyond 2070, global sea-level rise is a major source of uncertainty, which can potentially be reduced through research on Greenland and West-Antarctic ice sheets melting (Kopp et al., 2014). Conversely, studies focussing on local environmental decision making over the coming decades would require more information regarding sea-level variability.

Up to 2050, a large part of the uncertainties originate from the wave set-up. In many coastal hazard assessments studies, this process is often either neglected or incorporated uniformly into the reference water levels. However, the wave set-up contribution to high-water level can vary drastically in two neighbouring locations, depending on the local beach slopes.

A first approach to reduce the uncertainties due to wave set-up is to assume unchanged coastal bathymetry and to model it using advanced coastal hydrodynamic tools (Marche et al., 2007; Zijlema et al., 2011; Shi et al., 2012). If high resolution topo-bathymetric data such as LiDAR are available, such approach can be valid for the present situation. Such a study has been actually undertaken to evaluate marine flooding under several sea-level rise scenarios on our test site (Vinchon et al., 2011b). If we incorporate this study in the background knowledge (Table 2), this will lead to reduced uncertainties during the first years of simulations. However, after one or two decades, the range of possible set-up values will become as large as indicated in Table 2 again, due to submarine coastal evolution induced by sediment transport. Hence, the ranking of uncertainties will be unaffected after one or two decades. A long term coastal evolution model would be needed to anticipate changes of the coastal slopes. As reminded by Weisse et al. (2012), fundamental research on multi-decadal sediment transport is needed to gain insight into this source of uncertainty.

The relative importance of the climate change scenario becomes significant in the last decades of the 21st century. Hence, for this specific site, the benefits of climate change mitigation will be perceived late in the 21st century only. This reflects the fact that sea-level rise scenarios are very similar during the first part of the 21st century.

Whatever the research efforts, results will remain partly uncertain, just because the predictability of each of these processes is more or less limited. More observations and advanced modelling tools should help to reduce the uncertainties of parameters such as the contribution of ice-sheets to future sea-level rise, the regional variability of sea-level rise or the near-shore coastal evolution, but will certainly not decrease them up to zero.

4.3. Implications for adaptation

Our results have the potential to stimulate discussions on the most appropriate time-frame by which specific adaptation measures should be undertaken. If the decision is taken to maintain the coastal settlements, it is likely that defences will be progressively upgraded, but it is also likely that the willingness to fund them is bounded (Rulleau et al., 2014). If stakeholders concerned by coastal risks can define local acceptance levels for coastal flooding, Fig. 6 can be used to identify the period of time by which coastal maintenance should be undertaken. New simulations may indicate how long they will maintain the probability of flooding below the acceptance level.

The identification of such acceptance threshold is difficult and depends on numerous factors, including, cultural and sociological ones. For the present site considered, surveys have shown that this depends whether they are permanent or second-home residents (Rey-Valette et al., 2014). These surveys have indicated that in this particular area, about the half of the habitants could leave if they are flooded at least once a year (Data from Meur-Ferec et al., 2010 presented in Idier et al., 2013b), a situation which does not occur before the end of the 21st century according to our simulations. However, the observed attitude of individuals is different from their anticipated decision, and their attitude may also evolve over the time. In other contexts, there is evidence that the decision to abandon a coastal locality can take a long time before land has been definitively flooded (Arenstam Gibbons and Nicholls, 2006), whereas others have taken the decision to protect, whatever the costs. It seems therefore difficult to plan adaptation or resettlement strategies based on anticipated attitude of individuals toward changing coastal flooding risks at these timescales. Hence, considering the present knowledge available, we suggest that the social response to sea-level rise should be considered as an unquantifiable source of uncertainties that should be considered separately.

4.4. Implication for climate change mitigation

Fig. 6 clearly demonstrates the benefits of climate change mitigation on the long term: while the likely range of F_t rises drastically for RCP 6.0 and 8.0, it remains limited for RCP 2.6 (Fig. 6), suggesting that in this last case, several adaptation options are possible beyond relocation. However, because the probability distribution functions of the input parameters have been adjusted for a specific site, the details of our results would not be identical elsewhere. Still, for a first estimate, only the critical threshold should be reconsidered to extend this analysis to other urban coastal sites exposed to waves along the coastlines of the Gulf of Lion. Given the scale of the anticipated coastal changes, we also believe that in most low-lying areas exposed to flooding in the world, the ranking of uncertainties follows approximately the same chronological order. Interestingly, a shift toward increased vulnerability is projected by the end of the 21st century for several different coastal contexts, systems (beaches, inlets, wetlands, urban areas), and models, in particular for high sea-level scenarios (Purvis et al., 2008; Ranasinghe et al., 2013; Chu-Agor et al., 2014; Anderson et al., 2015). Collectively, all these results suggest that sea-level rise will generate numerous local pressures along the coastlines worldwide, at least if mitigation does not succeed to stabilize its rate. However, to verify these points, the method should be adapted to other coastal location, where basic information about coastal flooding hazards is available. Such repeated applications of similar approach at local to regional scales could further support the intuitive statement that for low-lying coastal zones, the RCP 2.6, and, possibly RCP 4.5, are the only targets where moderate (although potentially costly) adaptation efforts can be efficient with respect to sea-level rise.

The global sea-level rise scenarios used in this paper are based on those of IPCC (Church et al., 2013a). These scenarios have the advantage of relying on a large scientific consensus, which facilitates the process of stakeholders taking ownership of the results. However, this raises two difficulties: first, probabilistic parameters for IPCC sea-level rise scenarios are provided for the 21st century only, while only the model spread is available beyond 2100. Secondly, the boundaries of sea-level rise scenarios are not provided by IPCC (Church et al., 2013b), and must be evaluated from complementary knowledge. If we had used alternative data from e.g. Kopp et al. (2014) or from semi-empirical sea-level rise scenarios (Rahmstorf, 2007; Vermeer and Rahmstorf, 2009; Grinsted et al., 2010) instead of IPCC, the yearly probability of exceedance would have grown much more quickly (Fig. 6). Therefore, our sea-level rise scenarios (Fig. 4) could be optimistic, especially after 2100.

Collectively, all these points further support — if needed — the statement that the 2° C target should not be exceeded in order to avoid dangerous climate change. However, meeting this target requires serious and urgent measures in the coming decade (Guivarch and Hallegatte, 2013; Fabert et al., 2014).

5. Conclusion

This paper has undertaken a dynamic global sensitivity analysis of marine flooding to input parameters such as sea-level rise and local coastal processes. The method has been applied to the case of yearly probability of flooding in a Mediterranean coastal urban site located on a low-lying sand barrier. We have provided a quantified ranking of the relative importance of uncertainty factor, and we have identified which factor can be set without much impact for the final results. Coastal processes and particularly the wave set-up are dominant factors during the first part of the 21st century. Sea-level rise and climate change scenarios dominate by 2080. Sea-level rise variability has its maximum contribution to the uncertainties in-between these two periods. The uncertainties on the upper limit of sea-level rise projections is important a few decades later. However, the global sensitivity analysis gives a relatively low weight to this particular source of uncertainties, suggesting that the impacts of these low-probability and high-impacts scenarios should be evaluated independently. Our results illustrate that the temporal dimension of sea-level rise impacts would deserve more attention. Many studies focus on specified periods of time, such as, very often, 2030, 2070 or 2100. For our coastal site, this is exactly the period of time by which the frequency of flooding may start to grow drastically (Fig. 6).

Our results clearly discriminate the impacts of different climate change scenarios beyond 2100. For the site considered, only the RCP 2.6, and, perhaps, the RCP 4.5 scenarios are more than likely to lead to a manageable situation with moderate adaptation efforts. Other scenarios lead to sea-level changes higher than 1 m and create the conditions for repeated major disasters, thus making adaptation challenging and questioning about relocation and its planning. Given the geomorphological settings of the area — a low lying sand barrier located between the sea and coastal lagoon — one would expect such conclusion intuitively. Still, we provide quantified evidences of this statement.

From a methodological point of view, our application provides an example of a dynamic variance based sensitivity analysis that incorporates uncertainties on probabilistic laws parameters. There are few applications of global sensitivity analysis in the field of environmental change, and particularly in relation to sea-level rise impacts. However, it provides a quantitative and dynamic insight into the relative importance of each source of uncertainties, and the

results can be used for prioritizing research actions and to define impact assessment approaches adapted to the specific context of a given location, period of interest and amount of knowledge available. Therefore, we conclude by arguing that applying similar variance-based global sensitivity analysis would be very beneficial prior to any assessment of future marine flooding.

Acknowledgements

This research has been funded by BRGM (CCRA - Climate Change Risks and Adaptation project), with supplementary support from the French Ministry of Environment (Explore 2070 and ADAPT-MED CIRCLE-2 projects). We thank Alexis Stépanian, Pierre Sochala and Sylvestre Le Roy for many useful discussions and advices. We thank the Editor and three anonymous reviewers whose comments led to improving this article.

Appendix A. Global sea-level rise

Several different global sea-level rise projections are presently available (Church et al., 2013a). While some projections of sea-level rise have been provided in a probabilistic form (Kopp et al., 2014; Jevrejeva et al., 2014), this is only partly the case for those provided by the International Panel on Climate Change (IPCC). In the 5th assessment report, the IPCC provides the median and the likely range of sea-level changes up to 2100 for each scenario. This means a probability of 1/3 that sea-level rise exceeds or remains below this "likely" range (Church et al., 2013b). From 2100 to 2500, Church et al. (2013a) provides the spread of the model simulations. All these sea-level change values are provided for the four representative concentration pathways RCP 2.6, 4.5, 6.0 and 8.5. In our global sensitivity analysis, the representative concentration pathways (hereafter referred to as climate change scenarios) are selected by assuming equiprobability of all four climate change scenarios, following a procedure similar to Rohmer et al. (2014).

To undertake the global sensitivity analysis, a workable probabilistic model must be selected, that matches the boundary conditions provided by IPCC, as well as additional well established knowledge on future sea-level rise. Purvis et al. (2008) used a triangular law to represent the probability density function representing the global elevation of sea-level rise. However, recent research shows that an asymmetric distribution bounded by low-end or high end sea-level scenarios is preferable (Jevrejeva et al., 2014). Among the classical probability distributions functions, the Beta distribution has such a shape, as soon as its parameters α and β meet the condition $1 < \alpha < \beta$. The Beta distribution can be defined through its cumulative distribution function:

$$F(x;\alpha,\beta) = \frac{\int_0^x \theta^{\alpha-1}\cdot(1-\theta)^{\beta-1}\mathrm{d}\theta}{\int_0^1 \theta^{\alpha-1}\cdot(1-\theta)^{\beta-1}\mathrm{d}\theta} \quad (A.1)$$

where x is defined on [0,1].

Given low, high-end and median projections as well as their likely range, closed approximations of α and β can be found using Kerman's estimate of the median of Beta laws (Kerman, 2011), and then by solving numerically the equation:

$$F\left(h_{gslr}^{(UP_{likely})}(t,s_{rcp},z_{max}(t));\alpha,\beta\right) - F\left(h_{gslr}^{(LOW_{likely})}(t,s_{rcp},z_{max}(t));\alpha,\beta\right) = \frac{2}{3} \quad (A.2)$$

with $h_{gslr}^{(UP_{likely})}(t,s_{rcp},z_{max}(t))$ corresponding to the upper bound of the likely range of future sea-level rise for the climate change scenario s_{rcp} at time t under the assumption of a high-end sea-level scenario $z_{max}(t)$. To summarize, the IPCC medians and likely values and Equation (A.8) and Kerman's median formula are used to calculate unknown parameters of the Beta distribution (α and β) for the mid 21st century, 2100, and — with some assumptions — 2200. Low and high-end scenarios are used to scale the distributions boundaries. Using these formula, new scenarios following any assumptions as above can be generated automatically.

To complete the sea-level scenarios, we make additional assumptions:

- first, we linearly interpolate the *rates* of sea-level rise between each boundary conditions provided by IPCC for the 21st century, and a polynomial approximation was made to fit the more uncertain model spread results beyond 2100.
- Secondly, we assume that high-end scenarios by 2100 are uncertain and can vary from 1.5 to 3 m. Importantly, high-end scenarios are the same for all climate change scenarios in our simulations. This is justified by the fact that the west-Antarctica ice-sheet may have reached instability already, so that a rapid sea-level rise scenario can not be excluded even in case of scenario RCP 2.6. We assume a low-end scenario corresponding to the linear extrapolation of present observed sea-level rise rates.
- Third, we assume that the model spread provided by Church et al. (2013a) beyond 2100 corresponds to a likely range, as long as these values are plausible.

As a result, by the mid 21st century and for 2100, our global sea-level scenarios are strictly constrained by IPCC likely and median values. In addition, from now to 2100, Fig. 4 appears as a very close approximations of the IPCC Fig. 13.11 (Church et al., 2013a) displaying global sea-level rise likely and median projections for the 21st century.

A prerequisite for the application of the classical Sobol' estimator for the variance-based global sensitivity indices is the statistical independence of input parameters. However, in our application, global sea-level rise depends on the climate change scenario s_{rcp}. Following Sankararaman and Mahadevan (2013), we note that global sea-level rise can be computed as $F^{-1}(u_2|u_3,u_4)$ with F^{-1} the inverse cumulative distribution function of the Beta law, and u_2, u_3 and u_4 random variables uniformly distributed in [0,1] (see Fig. 5). In this case, u_2, u_3 and u_4 are independent variables and the global sensitivity analysis is applicable using common estimators.

Finally, our choice here is to strongly rely on IPCC, and to select values leading to moderate sea-level rise projections if this information is insufficient. This choice has been made considering that impacts are expected to be very large in this particular locality (Vinchon et al., 2011a). In such context, communicating coastal impact assessments scenarios above the widely agreed IPCC assessments is likely to raise doubts about the value of the results, and may finally lead to postpone actions in favour of adaptation or mitigation.

Appendix B. Regional variability

Compared to global sea-level rise, few indications are available to elaborate probability density functions representing sea-level variability. Sea-level rise regional variability can potentially account for 30% of the global mean in some regions. Presently, they are mostly due to unequal warming of the ocean surface, ocean circulation variability and the response of solid-Earth to past deglaciation. In the future, other processes will play a significant

role, in particular present days ice-sheets melting and the effects of mass redistributions to the gravity field. Further description of these processes can be found in Meyssignac and Cazenave (2012), Stammer et al. (2013), Tamisiea and Mitrovica (2011) and coupled simulations of this regional variability are provided in Slangen et al. (2014).

Based on the present knowledge of present and future regional sea-level variability in the considered area, we model it through three terms:

- a deviation from the global average: we use regional sea-level projection of Slangen et al. (2014), which anticipates a regional sea-level rise of +0.61 m by 2100 for RCP 8.5 in the north-western Mediterranean; considering the global sea-level projection of 0.71 m by 2100; this enables to introduce a scaling factor accounting for a predictable part of regional sea-level changes;
- a random contribution of sea-level regional variability, which we consider independent from the climate change and sea-level rise scenarios; this contribution represents steric sea-level changes; considering past modes of sea-level variability over the last 60 years (Meyssignac et al., 2012), we use Fig. 13.22 in Church et al. (2013a) and approximate the general shape of regional variability by a triangular probability density function of mean zero, with an amplitude growing progressively to 0.25 m over the next 65 years, and then remaining to this value.
- an inter-annual sea-level variability due to regional ocean circulation in this area, which we model though a triangular probability density function of mean zero and amplitude 0.1 m based on the analysis of tide gauge records of Marseille (http://refmar.shom.fr/marseille).

This results in a probability density function representing sea-level variability, which evolves over time as shown in Fig. B9.

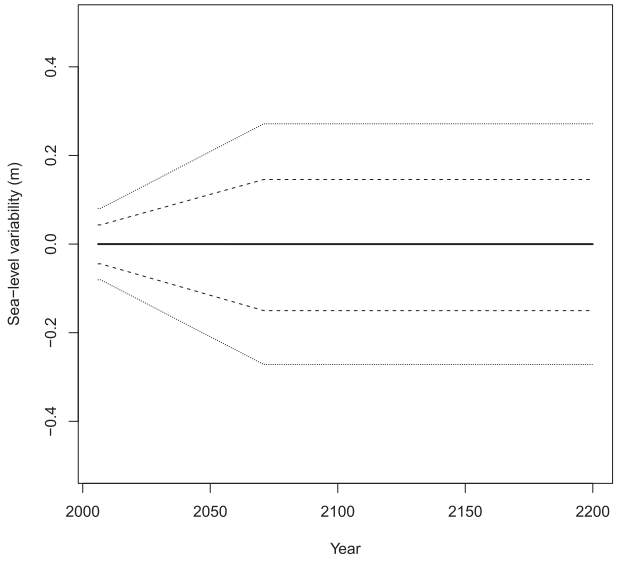


Fig. B9. Evolution over time of the probability density function representing sea-level variability. Solid, dashed and dotted lines correspond to the median, to likely (66%) and extremely likely (95%) ranges respectively. As a first approximation, we neglect the dependency between sea-level variability and the climate change scenarios.

Appendix C. Extreme water levels and waves set-up

Recommended practices for evaluating extreme water levels consists in undertaking a joint analysis of waves and offshore extreme water levels, or even river levels when appropriate (Hawkes et al., 2002). Such analysis requires long term consistent data or reanalysis, which were lacking in the present case when new reference values were defined to prepare regulatory coastal risk prevention plans. When such data are lacking, they form a source of uncertainties which largely oversteps those due to the choice of a modelling approach for extreme values analysis. They also dominate over any plausible change of marine storm climates in the Mediterranean (Ullmann, 2008).

In the present case, Equation (2) is simplified by considering the official evaluation of storm surge return periods (see Yates et al., 2011, and references therein), which relates directly extreme water levels to the vertical datum of the terrestrial framework (note that in this paper, all altitudes are given with respect to this datum, corresponding to mean sea-level in the harbour of Marseille). This allows to combine h_{pred}, ξ_{bar} and ξ_{wind} in Equation (2). Their sum is noted $h_{extreme}$ hereafter. Hence, we evaluate the variability of the two following terms underpinning the severity of extreme coastal water levels: the wave set-up and extreme water levels.

The French official recommendations lead to consider that events reaching 1 m and 2 m correspond to 10-years and 100-years events respectively. In areas exposed to waves, a reference value of 3 m should be considered. Considering the lack of available observations and the fact that the wave set-up is partly integrated in both reference values, we use water-levels ranging from 1.3 to 2 m for centennial events. We adjust a 2-parameters Pareto probability distribution function to these uniform random draws. Hence, the probability that $h_{extreme}$ exceeds a level h_{level} is:

$$F(h_{extreme} > h_{level}) = \left(\frac{\xi_m}{h_{level}}\right)^k \quad \text{(C.1)}$$

where the shape and scale parameters k and ξ_m can be easily calculated given the hypothesized extreme water levels, whose values are randomly chosen from a uniform distribution bounded by 1.3 m and 2 m for the centennial event, with the same proportion being applied for decennial events.

The wave set-up is a process that depends on bathymetric slopes and offshore waves and periods. It can be estimated using typical beach slopes, wave heights and periods (Gervais et al., 2012) and the Stockdon formula (Stockdon et al., 2006), or modelling and in-situ observations (Gervais, 2012). Using this approach, observational evidences and modelling leads to values ranging from 0.4 m to 0.8 m. As reminded above, a second source of uncertainties for the wave set-up is due to beach slopes evolving over the time, e.g. in response to natural processes, human actions, climate change and variability (e.g. Idier et al., 2013a). We consider as a first approximation that present-day variability of the wave set-up remains unchanged in the future, which is a conservative hypothesis, or may assume adaptation through beach nourishment.

References

Anderson, B., Borgonovo, E., Galeotti, M., Roson, R., 2014. Uncertainty in climate change modeling: can global sensitivity analysis be of help? Risk Anal. 34 (2), 271–293.
Anderson, T.R., Fletcher, C.H., Barbee, M.M., Frazer, L.N., Romine, B.M., 2015. Doubling of coastal erosion under rising sea level by mid-century in hawaii. Nat. Haz. 1–29.
André, C., 2013. Analysis of Dammages Due to Marine Flooding and Evaluation of Building Costs from Insurance Data: Perspectives from the Johanna (2008) and Xynthia (2010) Storms (In French) (PhD thesis).
Arenstam Gibbons, S.J., Nicholls, R.J., 2006. Island abandonment and sea-level rise: an historical analog from the Chesapeake Bay, USA. Glob. Environ. Change 16 (1), 40–47.
Bilskie, M.V., Hagen, S.C., Medeiros, S.C., Passeri, D.L., 2014. Dynamics of sea level rise and coastal flooding on a changing landscape. Geophys. Res. Lett. 41 (3), 927–934.
Brooks, B.A., Merrifield, M.A., Foster, J., Werner, C.L., Gomez, F., Bevis, M., Gill, S., 2007. Space geodetic determination of spatial variability in relative sea level

change, los angeles basin. Geophys. Res. Lett. 34 (1).
Bulteau, T., Idier, D., Lambert, J., Garcin, M., 2015. How historical information can improve estimation and prediction of extreme coastal water levels: application to the xynthia event at la rochelle (france). Nat. Haz. Earth Syst. Sci. 15, 1135–1147.
Campbell, K., McKay, M.D., Williams, B.J., 2006. Sensitivity analysis when model outputs are functions. Reliab. Eng. Syst. Saf. 91 (10), 1468–1472.
Cazenave, A., Le Cozannet, G., 2014. Sea level rise and its coastal impacts. Earth's Future 2 (2), 15–34.
Chu-Agor, M., Guzman, J., Muñoz-Carpena, R., Kiker, G., Linkov, I., 2014. A simplified approach for simulating changes in beach habitat due to the combined effects of long-term sea level rise, storm erosion, and nourishment. Environ. Model. Softw. 52, 111–120.
Chu-Agor, M., Muñoz-Carpena, R., Kiker, G., Emanuelsson, A., Linkov, I., 2011. Exploring vulnerability of coastal habitats to sea level rise through global sensitivity and uncertainty analyses. Environ. Model. Softw. 26 (5), 593–604.
Church, J., Clark, P., Cazenave, A., Gregory, J., Jevrejeva, S., Merrifield, M., Milne, G., Nerem, R., Nunn, P., Payne, A., Pfeffer, W., Stammer, D., U, A.S., 2013a. Sea level change, pages 1137–1216. In: Climate Change 2013: the Physical Science Basis. Contribution of Working Group I to the Fifth Assessment Report of the Intergovernmental Panel on Climate Change. Cambridge University Press, Cambridge, United Kingdom and New York, NY, USA.
Church, J.A., Clark, P.U., Cazenave, A., Gregory, J.M., Jevrejeva, S., Levermann, A., Merrifield, M.A., Milne, G.A., Nerem, R.S., Nunn, P.D., et al., 2013b. Sea-level rise by 2100. Science 342 (6165), 1445.
De La Torre, Y., Balouin, Y., Heurtefeux, H., Lanzellotti, P., 2013. The 'Storm Network' as a participative network for monitoring the impacts of coastal storms along the littoral zone of the Gulf of Lions, France. J. Coast. Res. 65 (Special Issue), 927–932. In: International Coastal Symposium (ICS) : 2013 Proceedings (Plymouth, United Kingdom).
Fabert, B.P., Pottier, A., Espagne, E., Dumas, P., Nadaud, F., 2014. Why are climate policies of the present decade so crucial for keeping the 2° C target credible? Clim. Change 126 (3–4), 337–349.
Fortunato, A.B., Rodrigues, M., Dias, J.M., Lopes, C., Oliveira, A., 2013. Generating inundation maps for a coastal lagoon: a case study in the Ria de Aveiro (Portugal). Ocean. Eng. 64 (0), 60–71.
Gamboa, F., Janon, A., Klein, T., Lagnoux, A., 2014. Sensitivity analysis for multidimensional and functional outputs. Electron. J. Stat. 8, 575–603.
Gervais, M., 2012. Impacts morphologiques des surcotes et vagues de tempêtes sur le littoral méditerranéen (PhD thesis, Perpignan). 370 p. and annex.
Gervais, M., Balouin, Y., Belon, R., 2012. Morphological response and coastal dynamics associated with major storm events along the Gulf of Lions coastline, France. Geomorphology 143, 69–80.
Grinsted, A., Moore, J.C., Jevrejeva, S., 2010. Reconstructing sea level from paleo and projected temperatures 200 to 2100 ad. Clim. Dyn. 34 (4), 461–472.
Guivarch, C., Hallegatte, S., 2013. 2C or not 2C? Glob. Environ. Change 23 (1), 179–192.
Hallegatte, S., 2009. Strategies to adapt to an uncertain climate change. Glob. Environ. Change 19 (2), 240–247.
Hallegatte, S., Green, C., Nicholls, R.J., Corfee-Morlot, J., 2013. Future flood losses in major coastal cities. Nat. Clim. Change 3 (9), 802–806.
Hanson, S., Nicholls, R., Ranger, N., Hallegatte, S., Corfee-Morlot, J., Herweijer, C., Chateau, J., 2011. A global ranking of port cities with high exposure to climate extremes. Clim. Change 104 (1), 89–111. Si.
Hawkes, P.J., Gouldby, B.P., Tawn, J.A., Owen, M.W., 2002. The joint probability of waves and water levels in coastal engineering design. J. Hydr. Res. 40 (3), 241–251.
Hemer, M.A., Fan, Y., Mori, N., Semedo, A., Wang, X.L., 2013. Projected changes in wave climate from a multi-model ensemble. Nat. Clim. Change 3 (5), 471–476.
Homma, T., Saltelli, A., 1996. Importance measures in global sensitivity analysis of nonlinear models. Reliab. Eng. Syst. Saf. 52 (1), 1–17.
Idier, D., Castelle, B., Poumadere, M., Balouin, Y., Bertoldo, R.B., Bouchette, F., Boulahya, F., Brivois, O., Calvete, D., Capo, S., Certain, R., Charles, E., Chateauminois, E., Delvallee, E., Falques, A., Fattal, P., Garcin, M., Garnier, R., Hequette, A., Larroude, P., Lecacheux, S., Le Cozannet, G., Maanan, M., Mallet, C., Maspataud, A., Oliveros, C., Paillart, M., Parisot, J.-P., Pedreros, R., Robin, N., Robin, M., Romieu, E., Ruz, M.-H., Thiebot, J., Vinchon, C., 2013a. Vulnerability of sandy coasts to climate variability. Clim. Res. 57 (1), 19–44.
Idier, D., Rohmer, J., Bulteau, T., Delvallée, E., 2013b. Development of an inverse method for coastal risk management. Nat. Haz. Earth Syst. Sci. 13 (4), 999–1013.
Jacques, J., Lavergne, C., Devictor, N., 2006. Sensitivity analysis in presence of model uncertainty and correlated inputs. Reliab. Eng. Syst. Saf. 91 (10), 1126–1134.
Jansen, M.J., 1999. Analysis of variance designs for model output. Comput. Phys. Commun. 117 (1), 35–43.
Jevrejeva, S., Grinsted, A., Moore, J.C., 2014. Upper limit for sea level projections by 2100. Environ. Res. Lett. 9 (10), 104008.
Kerman, J., 2011. A Closed-form Approximation for the Median of the Beta Distribution arXiv preprint arXiv:1111.0433.
Kopp, R.E., Horton, R.M., Little, C.M., Mitrovica, J.X., Oppenheimer, M., Rasmussen, D.J., Strauss, B.H., Tebaldi, C., 2014. Probabilistic 21st and 22nd century sea-level projections at a global network of tide-gauge sites. Earth's Future 2 (8), 383–406.
Le Cozannet, G., Garcin, M., Bulteau, T., Mirgon, C., Yates, M.L., Mendez, M., Baills, A., Idier, D., Oliveros, C., 2013. An AHP-derived method for mapping the physical vulnerability of coastal areas at regional scales. Nat. Haz. Earth Syst. Sci. 13 (5), 1209–1227.
Le Roy, S., Pedreros, R., André, C., Paris, F., Lecacheux, S., Marche, F., Vinchon, C., 2014. Coastal flooding of urban areas by overtopping: dynamic modelling application to the Johanna storm (2008) in Gavres (France). Nat. Haz. Earth Syst. Sci. Discuss. 2 (8), 4947–4985.
Lempert, R.J., Schlesinger, M.E., 2000. Robust strategies for abating climate change. Clim. Change 45 (3), 387–401.
Mara, T.A., Tarantola, S., 2012. Variance-based sensitivity indices for models with dependent inputs. Reliab. Eng. Syst. Saf. 107, 115–121.
Marche, F., Bonneton, P., Fabrie, P., Seguin, N., 2007. Evaluation of well-balanced bore-capturing schemes for 2d wetting and drying processes. Int. J. Numer. Methods Fluids 53 (5), 867–894.
Menéndez, M., Woodworth, P.L., 2010. Changes in extreme high water levels based on a quasi-global tide-gauge data set. J. Geophys. Res. Oceans 115 (C10).
Meur-Ferec, C., Flanquart, H., Hellequin, A.-P., Rulleau, B., 2010. ANR Miseeva, présentation des résultats Tâche 4.4 : Perception des risques (Palavas, Carnon, Mauguio). Technical report.
Meyssignac, B., Becker, M., Llovel, W., Cazenave, A., 2012. An assessment of two-dimensional past sea level reconstructions over 1950-2009 based on tide-gauge data and different input sea level grids. Surv. Geophys. 33 (5), 945–972.
Meyssignac, B., Cazenave, A., 2012. Sea level: a review of present-day and recent-past changes and variability. J. Geodyn. 58, 96–109.
Miller, A., Jonkman, S.N., Van Ledden, M., 2014. Risk to life due to flooding in post-Katrina New-Orleans. Nat. Haz. Earth Syst. Sci. Discuss. 2 (1), 825–864.
Muller, H., Pineau-Guillou, L., Idier, D., Ardhuin, F., 2014. Atmospheric storm surge modeling methodology along the French (Atlantic and English channel) coast. Ocean Dyn. 64 (11), 1671–1692.
Nicholls, R.J., Cazenave, A., 2010. Sea-level rise and its impact on coastal zones. Science 328 (5985).
Nicholls, R.J., Hanson, S.E., Lowe, J.A., Warrick, R.A., Lu, X., Long, A.J., 2014. Sea-level scenarios for evaluating coastal impacts. Wiley Interdiscip. Rev. Clim. Change 5 (1), 129–150.
Norton, J., 2015. An introduction to sensitivity assessment of simulation models. Environ. Model. Softw. 69, 166–174.
Pickering, M., Wells, N., Horsburgh, K., Green, J., 2012. The impact of future sea-level rise on the European shelf tides. Cont. Shelf Res. 35 (0), 1–15.
Purvis, M.J., Bates, P.D., Hayes, C.M., 2008. A probabilistic methodology to estimate future coastal flood risk due to sea level rise. Coast. Eng. 55 (12), 1062–1073.
R Core Team, 2014. R: a Language and Environment for Statistical Computing. R Foundation for Statistical Computing, Vienna, Austria.
Rahmstorf, S., 2007. A semi-empirical approach to projecting future sea-level rise. Science 315 (5810), 368–370.
Ranasinghe, R., Trang Minh, D., Uhlenbrook, S., Roelvink, D., Stive, M., 2013. Climate-change impact assessment for inlet-interrupted coastlines. Nat. Clim. Change 3 (1), 83–87.
Rey-Valette, H., Rulleau, B., Hellequin, A.-P., Meur-Férec, C., Flanquart, H., 2014. Second-home owners and sea-level rise: the case of the Languedoc-Roussillon region (France). J. Policy Res. Tour. Leis. Events 1–16 (ahead-of-print).
Rohmer, J., Douglas, J., Bertil, D., Monfort, D., Sedan, O., 2014. Weighing the importance of model uncertainty against parameter uncertainty in earthquake loss assessments. Soil Dyn. Earthq. Eng. 58, 1–9.
Rulleau, B., Rey-Valette, H., Hérivaux, C., 2014. Valuing welfare impacts of climate change in coastal areas: a French case study. J. Environ. Plan. Manag. 1–13.
Saltelli, A., 2004. Global sensitivity analysis: an introduction. In: Proc. 4th International Conference on Sensitivity Analysis of Model Output (SAMO'04), pp. 27–43.
Saltelli, A., Annoni, P., 2010. How to avoid a perfunctory sensitivity analysis. Environ. Model. Softw. 25 (12), 1508–1517.
Saltelli, A., Annoni, P., Azzini, I., Campolongo, Francesca, Ratto, M., Tarantola, S., 2010. Variance based sensitivity analysis of model output. design and estimator for the total sensitivity index. Comput. Phys. Commun. 181 (2), 259–270.
Saltelli, A., D'Hombres, B., 2010. Sensitivity analysis didn't help. a practitioner's critique of the stern review. Glob. Environ. Change-Human Policy Dimens. 20 (2), 298–302.
Saltelli, A., Ratto, M., Andres, T., Campolongo, F., Cariboni, J., Gatelli, D., Saisana, M., Tarantola, S., 2008. Global Sensitivity Analysis: the Primer. John Wiley & Sons.
Sankararaman, S., Mahadevan, S., 2013. Separating the contributions of variability and parameter uncertainty in probability distributions. Reliab. Eng. Syst. Saf. 112, 187–199.
Santamaria-Gomez, A., Gravelle, M., Collilieux, X., Guichard, M., Martin Miguez, B., Tiphaneau, P., Woeppelmann, G., 2012. Mitigating the effects of vertical land motion in tide gauge records using a state-of-the-art GPS velocity field. Glob. Planet. Change 98–99, 6–17. Santamaria-Gomez, Alvaro/E-4573-2013.
Shi, F., Kirby, J.T., Harris, J.C., Geiman, J.D., Grilli, S.T., 2012. A high-order adaptive time-stepping tvd solver for boussinesq modeling of breaking waves and coastal inundation. Ocean Model. 43, 36–51.
Slangen, A., Carson, M., Katsman, C., van de Wal, R., Köhl, A., Vermeersen, L., Stammer, D., 2014. Projecting twenty-first century regional sea-level changes. Clim. Change 124 (1–2), 317–332.
Sobol', I., 1967. On the distribution of points in a cube and the approximate evaluation of integrals. USSR Comput. Math. Math. Phys. 7 (4), 86–112.
Sobol, I., 2001. Global sensitivity indices for nonlinear mathematical models and their Monte Carlo estimates. Math. Comput. Simul. 55 (1–3), 271–280.
Stammer, D., Cazenave, A., Ponte, R.M., Tamisiea, M.E., 2013. Causes for contemporary regional sea level changes. Annu. Rev. Mar. Sci. 5, 21–46.

Stockdon, H.F., Holman, R.A., Howd, P.A., Sallenger Jr., A.H., 2006. Empirical parameterization of setup, swash, and runup. Coast. Eng. 53 (7), 573–588.
Tamisiea, M.E., Mitrovica, J.X., 2011. The moving boundaries of sea level change understanding the origins of geographic variability. Oceanography 24 (2), 24–39.
Tawn, J.A., 1992. Estimating probabilities of extreme sea-levels. Appl. Stat. 77–93.
Ullmann, A., 2008. Surcotes dans le Golfe du Lion et conditions atmosphériques: variabilité contemporaine et future (1900–2100). Université de Provence-Aix-Marseille I (PhD thesis).
Vermeer, M., Rahmstorf, S., 2009. Global sea level linked to global temperature. Proc. Natl. Acad. Sci. 106 (51), 21527–21532.
Vinchon, C., Angenais, A.L., Berthelier, E., Garcin, M., Grisel, M., Hérivaux, C., Kuhfuss, L., Maton, L., Meur-Ferec, C., Rey-Valette, H., et al., 2011a. Evolution of coastal zone vulnerability to marine inundation in a global change context. application to Languedoc Roussillon (France). In: Vulnérabilité des systèmes côtiers au changement global et aux évènements extrèmes.
Vinchon, C., Aubie, S., Balouin, Y., Closset, L., Garcin, M., Idier, D., Mallet, C., 2009. Anticipate response of climate change on coastal risks at regional scale in Aquitaine and Languedoc Roussillon (France). Ocean Coast. Manag. 52 (1), 47–56.
Vinchon, C., Baron-Yelles, N., Berthelier, E., Hérivaux, C., Lecacheux, S., Meur-Ferec, C., Pedreros, R., Rey-Valette, H., Rulleau, B., 2011b. Miseeva : Set up of a Transdisciplinary Approach to Assess Vulnerability of the Coastal Zone to Marine Inundation at Regional and Local Scale, within a Global Change Context.
Weisse, R., von Storch, H., Niemeyer, H.D., Knaack, H., 2012. Changing north sea storm surge climate: an increasing hazard? Ocean Coast. Manag. 68, 58–68.
Wong, P., Losada, I., Gattuso, J.-P., Hinkel, J., Khattabi, A., McInnes, K., Saito, Y., Sallenger, A., 2014. Coastal systems and low-lying areas, pages 361–409. In: Climate Change 2014: Impacts, Adaptation, and Vulnerability. Part A: Global and Sectoral Aspects, Contribution of Working Group II to the Fifth Assessment Report of the Intergovernmental Panel on Climate Change. Cambridge University Press, Cambridge, United Kingdom and New York, NY, USA.
Woodworth, P.L., Menendez, M., Gehrels, W.R., 2011. Evidence for century-timescale acceleration in mean sea levels and for recent changes in extreme sea levels. Surv. Geophys. 32 (4–5), 603–618.
Woppelmann, G., Le Cozannet, G., de Michele, M., Raucoules, D., Cazenave, A., Garcin, M., Hanson, S., Marcos, M., Santamaria-Gomez, A., 2013. Is land subsidence increasing the exposure to sea level rise in Alexandria, Egypt? Geophys. Res. Lett. 40 (12), 2953–2957.
Yates, M.L., Le Cozannet, G., Lenotre, N., 2011. Quantifying errors in long-term coastal erosion and inundation hazard assessments. J. Coast. Res. 260–264.
Zijlema, M., Stelling, G., Smit, P., 2011. Swash: an operational public domain code for simulating wave fields and rapidly varied flows in coastal waters. Coast. Eng. 58 (10), 992–1012.